

Dry Separation of Brown Coal Fly Ash, Determination of Properties of Separated Parts, and Their Application in High Volume Cementitious Pastes

Usman Haider^{1*}, Zdeněk Bittnar¹, Asif Ali², Lubomír Kopecky¹, Vít Šmilauer¹, Petr Bittnar¹, Jaroslav Pokorný³

Received 03 February 2016; Revised 21 April 2016; Accepted 20 June 2016

Abstract

The dry separation of brown coal fly ash was carried out in this research using ultrafine air classifier. Classifiers wheel speed was increased from 2000 to 10000 rpm to obtain fine and coarse products. As the speed of classifier was increased diameter of particles decreased and particle morphology was observed on optical, electron microscopes which showed that at 10000 rpm classifiers wheel speed, average fine particles morphology changed from angular and rounded irregular slaggy particles to spherical particles. High volume cementitious mixes were prepared with fine and coarse products in which cement – 60% fine products samples showed a considerable increase of compressive strength as compared to cementitious raw fly ash control samples.

Keywords

fly ash, dry separation, wheel speed, fine and coarse products, morphological, and particle size

1 Introduction

Coal fly ash is a waste by-product from the point of view of electricity generation while from the perspective of utilization it is a resource yet to be fully utilized [1]. Fly ash is registered as a useful chemical substance according to REACH (European regulation on Registration, Evaluation, Authorisation and Restriction of Chemicals) having several applications [2] but still its utilization is 25% globally [3]. Therefore thermal energy producers are looking for ways to increase the utilization of fly ash [4]. There are various reasons to increase the utilization of fly ash for e.g. disposal costs of fly ash can be minimized, less area is reserved for disposal, financial returns from the sale of fly ash, and fly ash can replace natural resources [5].

Grinding and classifying methods are usually adopted for adjusting the particle size of fine powdery materials such as fly ash [6]. Grinding of fly ash is usually employed to decrease the size of particles, and to increase the surface area thereby increasing the hydration activity with cementitious materials to increase the utilization of fly ash [7]. Morphologically fly ash particles consist of hollow spheres, compact spheres and slaggy / irregular particles [8-10]. Each type of fly ash particle possess its own physical properties, mechanical grinding force during grinding process usually destroys the morphological and networking structure of fly ash particles thereby accumulating all morphological types of fly ash particles into finer fraction [11]. However, classifying separation of fly ash particles is a method in which actual structure of fly ash can be preserved and simultaneously the size of particles can be adjusted which can be used for increasing the hydration activity when mixed with cementitious materials.

Application of all morphological type of particles are not desired in many applications, one morphological type out of other morphological types of fly ash particles is more important in certain applications than others, which makes the utilization of fly ash as a whole difficult in many applications [12]. Wet separation of fly ash to recover certain type of fly ash spherical particles from other fly ash particles have been carried out from the fly ash lagoons using water by [13, 14] and using Lithium Metatungstate solution by [15] because of their wide

¹ Department of Mechanics, Czech Technical University in Prague, Czech Republic

² Department of Chemical Engineering, University of Engineering and Technology, Lahore, Pakistan

³ Department of Material Engineering and Chemistry, Czech Technical University in Prague, Czech Republic

* Corresponding author, e-mail: usmanhaider6886@gmail.com

range of applications [16]. However wet fly ash separation methods consumes considerable expensive land for building ponds and have associated hazards of air and water pollution caused by fly ash particles [17, 18]. Air classifiers can be used to separate particles of fly ash based on density separation of fly ash particles. Galperin and Shapiro 2005 investigated the performance of different type of air classifiers and showed that the principle of density separation is based on the fact that the particles experience gravity and drag forces acting in opposite directions in the classifiers. Heavy particles with terminal settling velocity larger than the velocity of air move downwards while the light particles move to the top of the column [19]. Hirajima et al 2010 used an air classifier / micron separator from Hosokawa Micron Company to carry out dry separation of fly ash. The separation was carried out with rotor speed of 600, 1000, 1600, 1800 and 2200rpm. Overflow and underflow products were obtained where microspheres recovery from fly ash was the primary objective [20]. Similarly Petrus et al 2011 carried out dry separation with a closed type pneumatic separator and a micron separator for microspheres recovery [21]. Initially free vortex air classifiers were developed industrially in which the cut points were strongly influenced by product to air ratios and particle size was difficult to control, however cut point dependence on product to air ratio can be avoided by using the forced vortex air classifiers where circumferential velocity depends on rotor speed which allows adjusting particle size within 20 μm [22].

Brown coal fly ashes usually have very less percentage of microspheres, lesser binding properties, represent around half of the fly ash generated globally [23] and to increase the utilization of these fly ashes is a challenge for which classifying methods are required to adjust the particle size. In this research brown coal fly ash is used in an improved air classifier manufactured by Hosokawa Alpine, Germany to adjust the size of fly ash particles in a way to obtain morphologically suitable fly ash particles to be used in cementitious mixes. This classifier is an optimized model of air classifier, as compared to [20] and [21] from Hosokawa company, based on the principle of forced vortex and providing better control over the size of particle with cut point of 5 μm having new feature of spiral secondary air to separate all possible fine particles within certain range from the coarse particles. The purpose of this research is to carry out dry separation of fly ash particles using air classifier to study the morphology of fly ash particles before and after separation and to determine the physical and chemical properties of separated fly ash particles. Moreover dry separation of fly ash carried out by [20–23] did not consider into account the effects of adding separated fractions of fly ash in cementitious binders on their mechanical properties. Therefore this research focusses on adding the products obtained from the air classifier in cement to test for the properties of hardened separated fly ash – cement paste mixes to analyse the potential of separated

brown coal fly ash to be used in cementitious composites. Further to develop the relationship between particle size of fly ash and compressive strength of mixes achieved for establishing design equations.

2 Materials and Methods

2.1 For dry separation of raw fly ash

2.1.1 Dry separation using classifier

Dry separation of brown coal fly ash from Počerady power plant of Czech Republic was carried out using ultrafine air classifier manufactured by Hosokawa Alpine, Germany. Fig. 1 shows the classifier and description of its parts.



Fig. 1 Alpine Turboplex - Ultrafine Classifier 50 ATP, prepared in collaboration with [26]

Raw fly ash was fed into the classifier's top section, by opening the feed screws. The air-classification took place according to the principal of forced vortex by the use of a deflector turbine wheel and/or by the variation of the volume of the classifying air. Fine and coarse products were obtained and fineness of fines from fly ash was controlled by adjusting the classifier wheel speed at an increment of 2000 rpm from 2000 to 10000 rpm from the control panel. The fine products flowed upwards with the classifying air through the classifying chamber into the fine material zone through the classifying wheel while an air purged fines outlet prevented the entry of oversized materials. Whereas the coarse products were separated by the classifier which gravitated downwards through the coarse material classifying zone, closer to the wall of classifier, in the bottom part of the classifier. At the bottom part coarse fraction was intensively dispersed by the spiral secondary air inserted from three sides of the classifier because in a forced vortex peripheral speed is zero at the centre and is proportional to the radius. Therefore to overcome this, secondary air was employed to create another forced vortex inside the centre of primary forced vortex to enhance the removal of any finer particles which fall within the centre of the primary forced vortex as shown in Fig. 2.

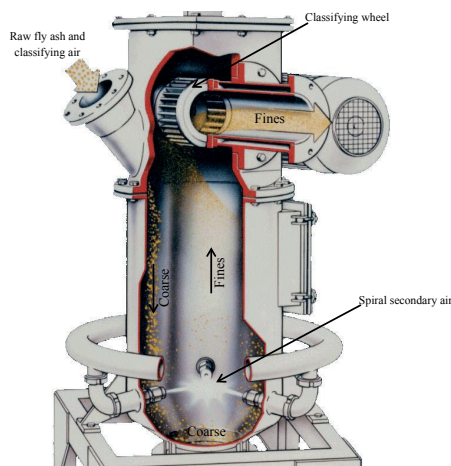


Fig. 2 Classifier's internal view, prepared in collaboration with [26]

In this phase the remaining fines were exposed and they finally entered through the classifier wheel at the top of classifier to the fine product zone whereas the extremely cleaned coarse material fraction left the classifier after passing the settling tank via an airlock. This classifier offers two parameter's for increasing the fineness of the fine products, classifier wheel speed and air flow. One parameter was kept constant to increase the other for increasing the fineness of fine products. For this research, only wheel speed was increased to increase the fineness of fines. Wheel speed and air flow has considerable effect on the fineness and capacity of fine products obtained. Higher the wheel speed, higher the fineness and lower the capacity of fines obtained and vice versa. Table 1 summarizes the effect of wheel speed and air flow on fineness and capacity of fines obtained.

Table 1 Effect of wheel speed and air flow on fineness and capacity of fines

Wheel Speed	Air Flow	Fineness	Capacity
Constant	Constant	Constant	Constant
High	Constant	High	Low
Low	Constant	Low	High
Constant	High	Low	High
Constant	Low	High	Low

2.1.2 Physical properties

Particle size analysis of separated / classified samples of fly ash was carried out on Fritsch particle size analyser and for comparison with separated fly ashes cement, EN 197-1, CEM I 42.5 R was used. Density of each separated part of raw fly ash was determined using Helium Pycnometer after complete removal of moisture by oven drying the specimens. Specific surface area of samples was measured using Blaine fineness analyser. Optical images of particles were observed and sizes of particles were measured on optical microscope manufactured by Zeiss, Germany for raw fly ash and coarse and fine products at 2000, 4000, 6000, 8000 and 10000 rpm.

Field emission electron microscope (FE-SEM) manufactured by Zeiss, Germany operated at an acceleration voltage of 30 kV was used under high vacuum conditions to determine morphology of fly ash particles and images were captured by HE-SE detector. Analyses were carried out by EDX software AZtec-Energy by oxford instruments to determine the chemical composition of elements present in separated fly ash specimens for only coarse and fine products obtained at 8000 and 10000 rpm.

Samples for FE-SEM testing were prepared with 1 to 3 ratio of solution of Araldite 2020/A epoxy resin to Araldite 2020/B hardener with two drops of Xylen solution in 50 ml solution. The epoxy mixture added with specimens were heated to 40°C for 2 min to give mixture a lower viscosity, thereby ensuring thorough penetration into the pores of the specimen. Then to remove air bubbles from the samples they were vacuum impregnated at 0.17 bar pressure for 2 hours in Struers Citovac vacuum impregnation machine. Following impregnation, specimens were left for 48 hours to be hardened and then specimens were cut to the required shape and were brushed and diamond polished on Struers, Tegramin-25 machine. Following the polishing, specimens were carbon coated to a thickness of 12.8nm with Quorum Q150R ES pumped sputter carbon coater.

2.2 For cement modified with fly ash and its separated fractions

For compressive strength testing, specimens of size 50 × 50 × 50 mm were prepared in accordance with ISO 1920 with up to 60% cement replacement by weight with 2000 to 10000 rpm fine products, 2000 to 10000 rpm coarse products, and control specimen with raw fly ash. Samples were prepared each with water/cement ratio of 0.4. Mixing was carried out according to EN 480-1 and cement EN 197-1, CEM I 42.5 R was used in the preparation of mixes. Brown coal raw fly ash from Počerady power plant of Czech Republic was used in control mixes. One day after preparation of specimens moulds were opened and samples were cured for 28, 90 days in water before further testing.

3 Results & Discussion

3.1 For dry separation of raw fly ash

3.1.1 Physical properties

Particle size is an important physical property of particulate samples. Particle size distribution measurements are regularly carried out by several industries as it indicates quality and performance and has strong influence on properties of materials and is a critical parameter in products manufacturing [24–25]. In this research particle size distribution was carried out to compare the differences in particle sizes of raw fly ash and fine, coarse products obtained after separation of fly ash from the classifier at 2000, 4000, 6000, 8000, and 10000 rpm revolution speeds of classifying wheel. The cumulative particle size distributions curves were plotted from the results of particle sizes analyser as shown in Fig. 3 and Fig. 4. In Fig. 3 the cumulative

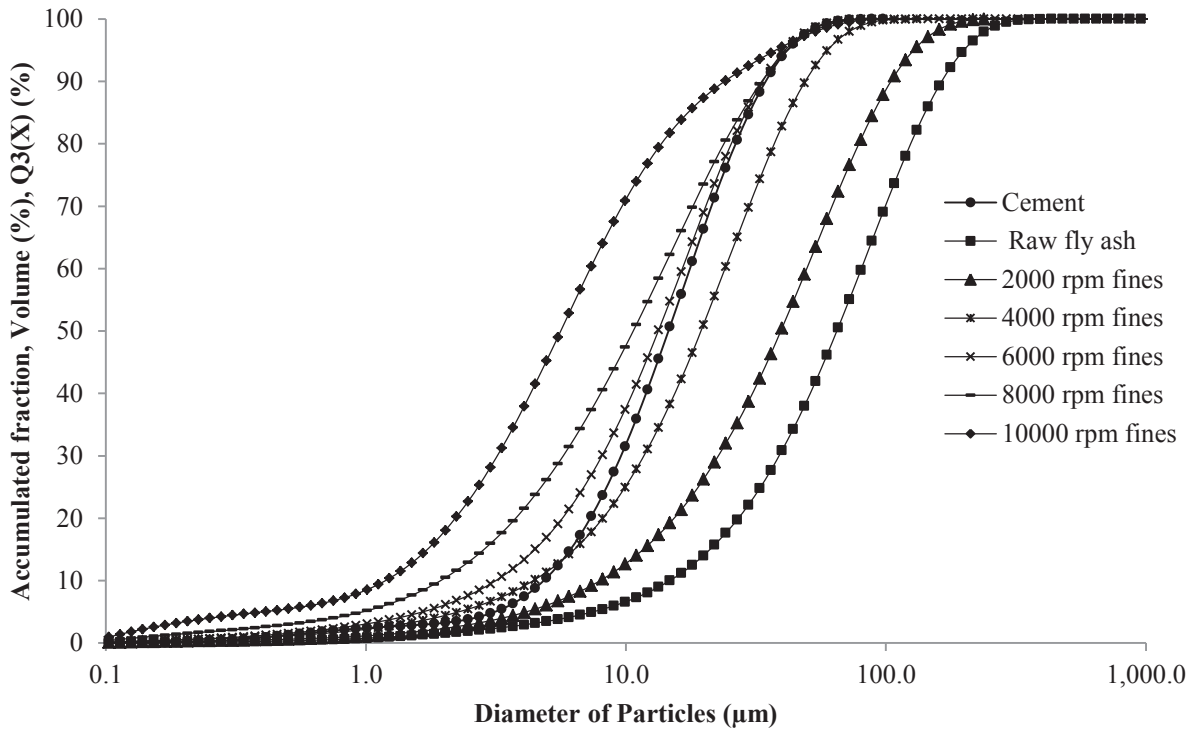


Fig. 3 Cumulative particle size distribution comparison of cement, raw fly ash, 2000 to 10000 rpm fine products

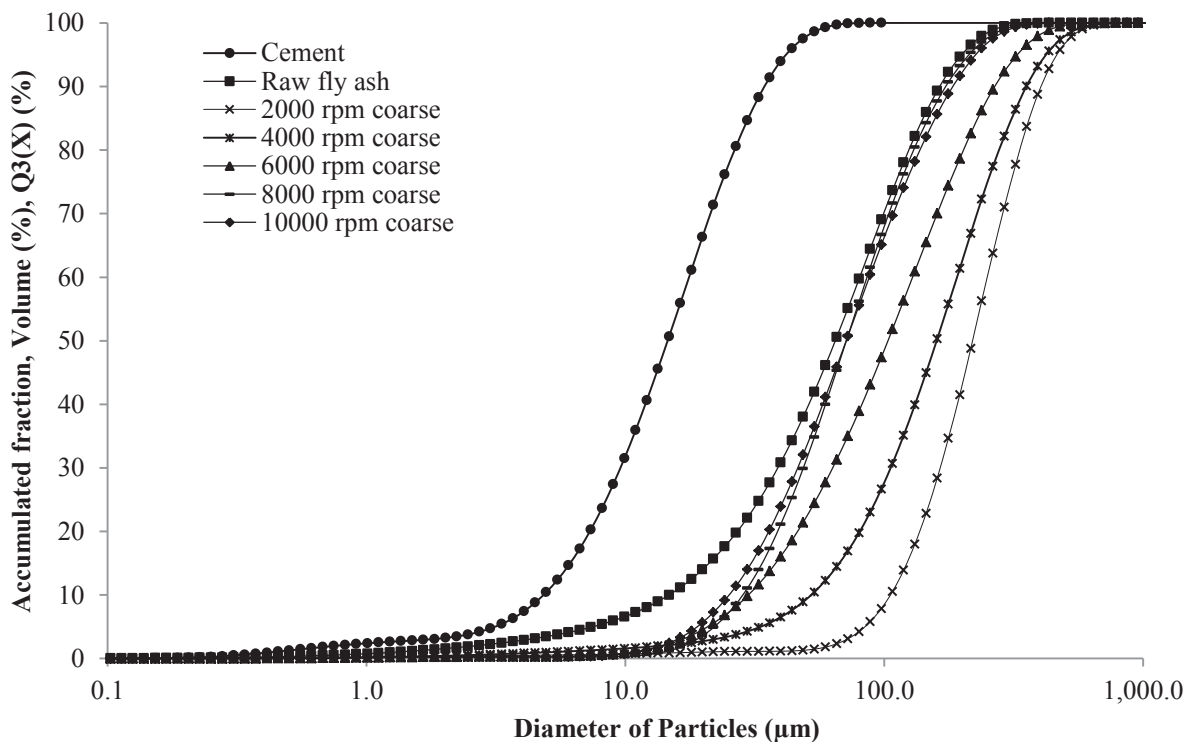


Fig. 4 Cumulative particle size distribution comparison of cement, raw fly ash, 2000 to 10000 rpm coarse products

distribution curves of fine products obtained at 2000 to 10000 rpm wheel revolution speeds is presented and compared with raw fly ash and cement. It can be seen here that raw fly ash has the coarsest particle size distribution as its curve is at the right most side of the remaining curves while distribution of cement particles is very closer to the curve obtained for fines at 6000 rpm revolution speed of classifying wheel and finest curve on the left most side is obtained for the 10000 rpm fines. Moreover it is clearly seen that as the wheel revolution speed is increased more fine cumulative distributions results.

Similarly Fig. 4 shows cumulative distribution for coarse products obtained from classifier at 2000 to 10000 rpm wheel speed along with distributions of raw fly ash and cement. It can be seen from Fig. 4 that 2000 rpm coarse have the coarsest particle size distribution while particle size distribution of raw fly ash and 10000 rpm coarse are very close to each other, whereas cement shows finer distribution as compared to raw fly ash and any of coarse products. It can be seen clearly that as the wheel speed is increased from 2000 to 10000 rpm, coarse products show finer distributions.

Fig. 5 shows the measures of central tendency and distribution widths. Fig. 5(a) shows relationship between d_{25} and classifiers wheel speed, it can be seen here that as the classifier is operated at a minimum speed of 2000 rpm there is a sudden change in diameter of particles and d_{25} for coarse particles increase considerably while for fine particles it decreases. But as the classifier wheel speed is increased d_{25} for both fine and coarse products decrease. Similarly Fig. 5(b) shows relationship between median diameter d_{50} and classifiers wheel speed and similarly it can be seen here that at wheel speed of 2000 rpm there is a sudden change of particle diameter as compared to that of raw fly ash. At 2000 rpm the median diameter, d_{50} for coarse products increased considerably by 265% as compared to that of raw fly ash where as a decrease of median diameter of 52% is seen for fine products. While by increasing the wheel speed from 2000 to 10000 rpm a decrease in particle diameter is seen both for coarse products as well as for fine products and at wheel speed of 10000 rpm for coarse products an increase of 19% of median diameter is seen as compared to raw fly ash while at this wheel speed for fine products a decrease of 90% of particle diameter is seen as compared to median diameter of raw fly ash and minimum median diameter of $5.62 \mu\text{m}$ is obtained. However, as wheel speed is increased from 8000 to 10000 rpm, a further decrease in particle size is not observed for coarse products but a little decrease in diameter is observed for fines. Above the speed of 10000 rpm either all the particles of raw fly ash were moved to the coarse products zone or the particles obtained at greater speeds had nearly the same sizes as obtained at the speed of 10000 rpm. Upper limit diameter, d_{97} determines the upper limit of particle size distribution and is a useful industrial measure [28] to compare the sizes of fine materials.

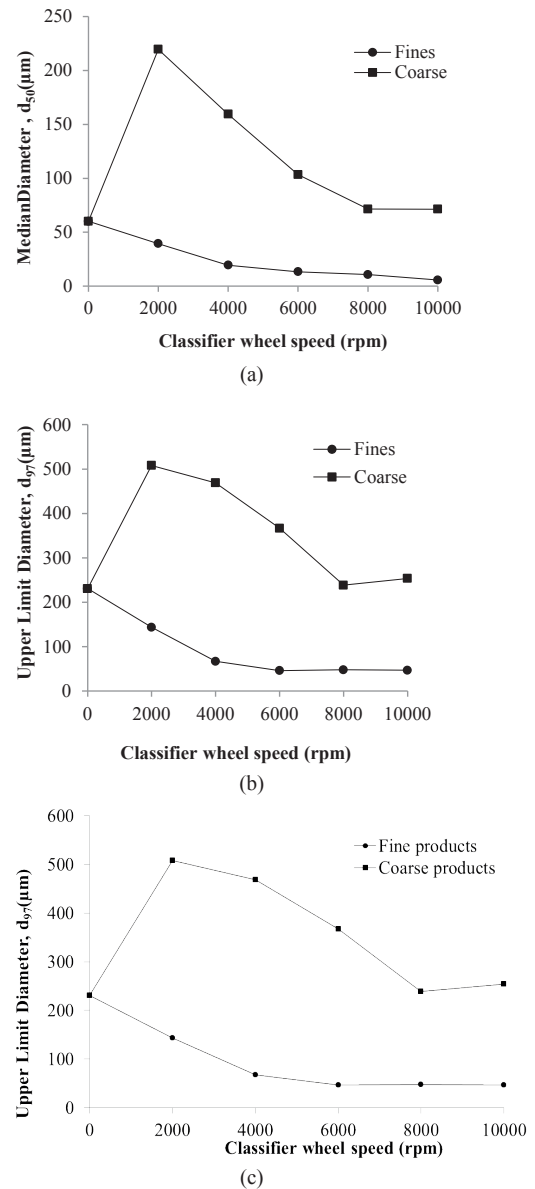
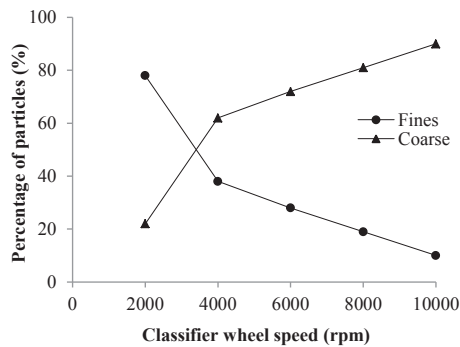
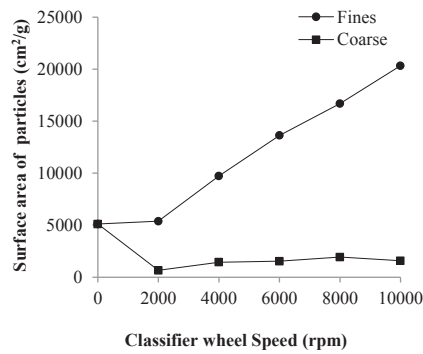


Fig. 5 Diameter, d_{25} vs classifier wheel speed (a) Median Diameter, d_{50} vs classifier wheel speed (b), Upper limit diameter, d_{97} vs classifier wheel speed (c)

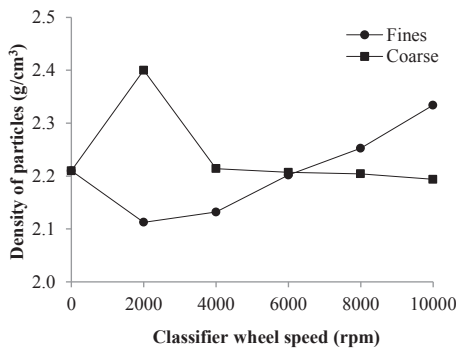
A similar trend of upper limit diameter is also seen as that of median diameter, when the wheels speed is increased from 2000 to 10000 rpm as shown in Fig. 5(c). This shows that at 2000 rpm wheel speed, the median diameter changes significantly and a very high rise in median and upper limit diameter is seen for coarse products as compared to fine products. Which shows that at 2000 rpm wheel speed only the coarsest particles in raw fly ash are separated because at a lower speed, mass force exerted by the peripheral velocity of classifying wheel is low, therefore only coarsest particles are rejected to the coarse products bin. While the remaining fine particles influenced by the drag force of the fluid travel through the classifier wheel into fine products zone [27]. However, as the classifier wheel speed is increased, the peripheral velocity of the wheel increases the mass forces on the particles, while drag force due to fluid stays the same and as a result more particles are rejected and only finest fine fraction due to drag force enter the fine products zone [27].



(a)



(b)



(c)

Fig. 6 Percentage of particles vs Classifier wheel speed (a), Surface area of particles vs Classifier wheel speed (b), Density of particles vs Classifier wheel speed (c)

Fig. 6(a) shows the percentage of coarse and fine products recovered against the classifiers wheel speed. It can be seen here that as the classifiers wheel speed is increased from 2000 to 10000 rpm, percentage of fine products recovered decreases, while the percentage of coarse products recovered increases. Moreover it can be seen that for a certain wheel speed, for e.g. at 10000 rpm, 90% coarse products were recovered while only 10% fine products were recovered which signifies that raw fly ash contains in it only 10% particles of sizes obtained at 10000 rpm classifiers wheel speed for fine products.

Fig. 6(b) shows the specific surface area of coarse and fine products against the classifiers wheel speed. It can be seen here that as the classifiers wheel speed is increased, the specific surface area of the fines increase considerably and maximum specific surface area for fine products is obtained at the classifier

wheel speed of 10000 rpm while for coarse products minimum surface area is obtained at 2000 rpm wheel speed, following it as the classifiers wheel speed is increased from 2000 rpm to 10000 rpm, particle size of fly ash decreases due to which specific surface area increases as also determined by [28].

Fig. 6(c) shows the density of coarse and fine products against the classifiers wheel speed. It can be seen in this figure that for coarse products and fine products a sudden change of density is seen between 0 and 2000 rpm wheel speed, a significant increase in density is seen for coarse products, while a less significant decrease of density is seen for fine products. As already explained that median diameter for coarse products increased by 265%, whereas median diameter decreased by 52% for fine products between 0 and 2000 rpm wheel speed. As the particle diameter significantly increased for coarse products which in turn significantly increased the density of particles and vice versa happened for fine particles. However as the classifiers wheel speed is increased from 2000 to 10000 rpm, for coarse products the density gradually decreases whereas for fine products density gradually increases and at 6000 rpm wheel speed almost same density of particles is achieved for both fines and coarse products. The gradual decrease of density of coarse products is due to the phenomenon that as the classifier wheel speed was increased, particles from fine products were being rejected and were transferred to coarse products zone, having lesser densities as compared to particles already present in coarse products zone, and hence started to decrease the density of resulting coarse products. While on the other hand as the wheel speed is increased, the density of fine products is increasing because the lighter particles bigger in size are transferring to the coarse material zone and leaving behind only fine fraction lesser in size having higher density.

3.1.2 Morphological Properties

Measurements of particles carried out by particle size analysers are based on the assumption that particles are spherical in shape and diameters recorded and reported are equivalent spherical diameters of particles [29]. However particles can have many different shapes and sizes other than being only spherical, therefore to determine the shape of particles, microscopic examination at different magnifications was carried out. Optical microscopic images were observed at 10 X magnification for raw fly ash, fine products, and coarse products obtained after separation as shown in Fig. 7. Fig. 7(a) shows that raw fly ash particles consist of spherical particles of radial size measured up to 149 μm , and slaggy particles of sizes measured up to 347 μm as also determined by [30].

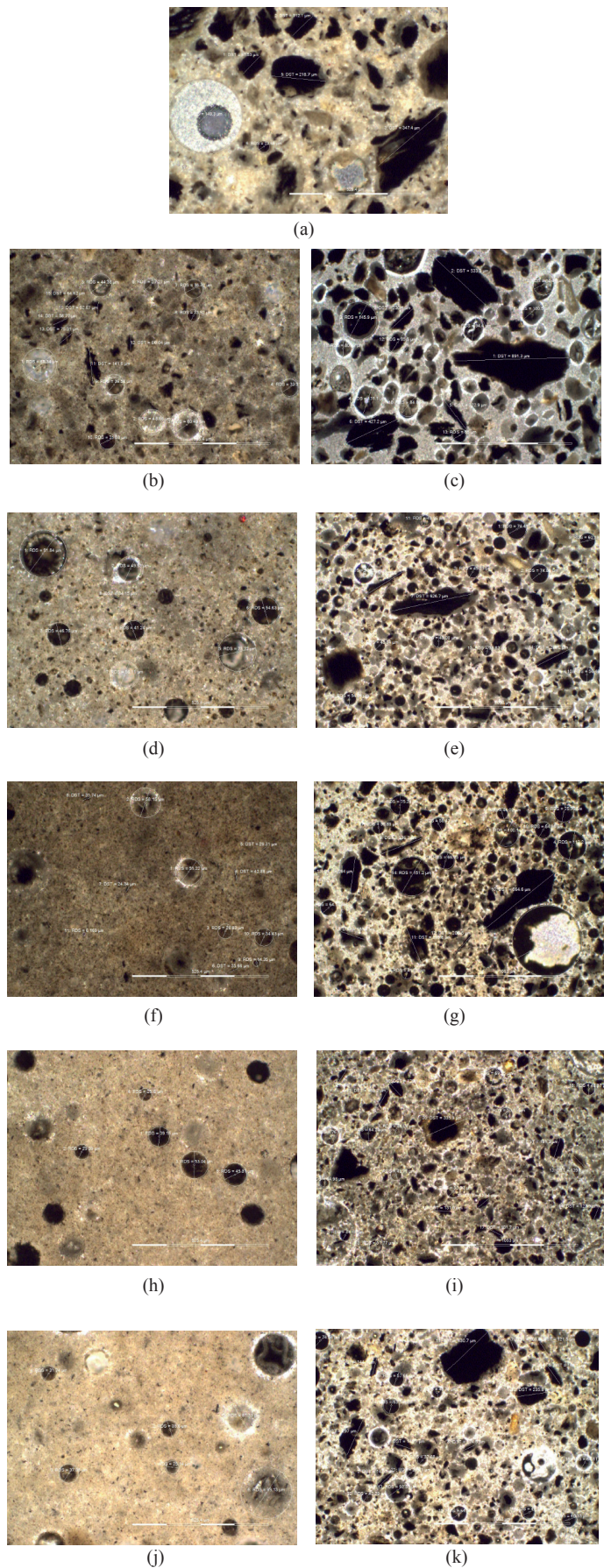


Fig. 7 Optical microscopic images at 10 X magnifications for raw fly ash (a), 2000 rpm fines (b) and coarse (c), 4000 rpm fines (d) and coarse (e), 6000 rpm fines (f) and coarse (g), 8000 rpm fines (h) and coarse (i), 10000 rpm fines (j) and coarse (k)

Fig. 7 (b), (d), (f), (h), and (j) shows optical images of fine products recovered from the classifier at 2000, 4000, 6000, 8000, and 10000 rpm wheel speeds, the images shows that they consist of spherical particles of radial size measured up to 68.3, 54.6, 58.2, 53, and 37 μm , and slaggy particles of sizes measured up to 141.8, 34.2, 24.3, 18.8, and 11.9 μm . It can be seen here clearly that as the classifier wheel speed is increasing, the particle size is decreasing and particle size of slaggy particles decrease considerably as compared to spherical particles. The reason for comparatively lesser decrease of particle size of spherical particles is that the spherical particles are mostly hollow also known as cenospheres [31] and have very less density compared to other fly ash particles. However, as the classifiers wheel speed is increased the mass forces on the particles increases and rejects coarser and relatively more dense particles, while drag force due to air fluid in classifier carries comparatively less dense hollow spheres along with other fine fly ash particles to the fine products chamber.

Similarly Fig. 7 (c), (e), (g), (i), and (k) shows optical images of coarse products recovered from the classifier at 2000, 4000, 6000, 8000, and 10000 rpm classifiers wheel speed. The particles in these images consist of spherical particles of radial sizes measured up to 145.9, 90.7, 275.5, 76.6, and 92.5 μm , and slaggy particles of sizes measured up to 891.3, 626.7, 664.6, 336, and 430.7 μm . It can be seen in these optical microscopic images that as the classifier speed is increasing fine particles are being added to the coarser fraction, and coarser fraction is being filled by the finer fraction therefore only fewer particles with large sizes can be seen. A decrease in particle size for slaggy particles is observed but much change is not observed for spherical particles. The reason for increase of finer fraction in coarse products as speed is increased is because of the increase of mass force on the particles which rejects coarser particles from finer fraction which then enters the coarse products zone and joins the much large size coarser already rejected particles in the coarse products zone.

It can be seen from optical microscopic images of Fig. 7 that as the classifiers wheel speed is increased, the fine products are getting finer and at low magnification of optical microscope it is not easy to see the particle morphology clearly. To overcome this fine and coarse products obtained at 8000, 10000 rpm classifiers wheel speed were tested under field emission electron microscope at higher resolutions. Fig. 8 shows the results of fine and coarse products obtained at 75 X magnifications. Fig. 8 (a) and (c) shows fine products in which only spherical particles can be seen and other finer particles are not seen at this magnification, the spheres that can be seen are mostly hollow. As the classifier speed is increased from 8000 rpm to 10000 rpm, diameter of spheres is reducing for fine products.

In Fig. 8 (b) and (d) morphology of coarse products at 8000, 10000 rpm classifier wheel speed is shown which shows that coarse products contain mainly hollow spherical, compact

spherical, compact slaggy, porous spherical, porous slaggy particles, and some brighter particles compared to other particles can also be observed also identified by [32]. Furthermore it can be seen that as the classifiers wheel speed is increasing, finer particles as compared to already available coarse particles are being added to the coarse products, which include greater quantity of hollow spheres rejected from the fine products, which are primarily responsible for lower density of the coarse products.

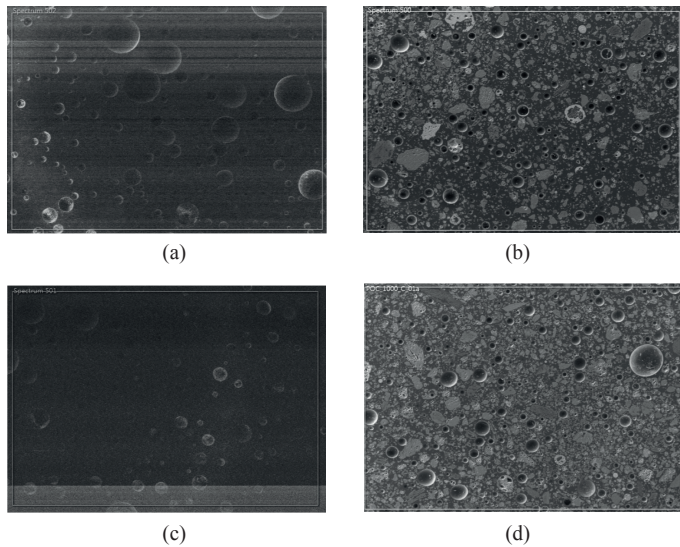


Fig. 8 Electron microscopic images at 75 X magnifications for 8000 rpm fines (a), 8000 rpm coarse (b), 10000 rpm fines (c), 10000 rpm coarse (d)

Magnification was increased to clearly identify the morphology of particles, for this fine products at a magnification of 2.5 KX were obtained as shown in Fig 9 (a) and (c). Fine products obtained at 8000 rpm classifiers wheel speed at 2.5 KX magnification in Fig. 9 (a) shows mostly glassy, slaggy, porous rounded shape particles, compact and hollow spherical particles can also be seen but are small in number as compared to rounded slaggy particles, and very few angular slaggy particles are seen. However fine products obtained at 10000 rpm classifiers wheel speed at 2.5 KX magnification in Fig. 9(c) shows majority of compact and hollow spherical particles, whereas slaggy rounded shape particles are seen to be very few in number, and angular slaggy particles are absent from this image. On the other hand Fig. 9 (b) and (d) shows coarse products at 8000, 10000 rpm wheel speed at a magnification of 500 X. At 8000 rpm classifiers wheel speed in Fig 9 (b), the coarse products obtained are seen to be mostly angular and slaggy, some rounded and slaggy, few compact and hollow spherical, and few bright spherical particles of different sizes. In comparison to this in Fig. 9 (d) more hollow and compact spherical particles can be seen along with rounded and angular slaggy particles, and more inter particle spaces are filled by finer particles which are rejected from fine products.

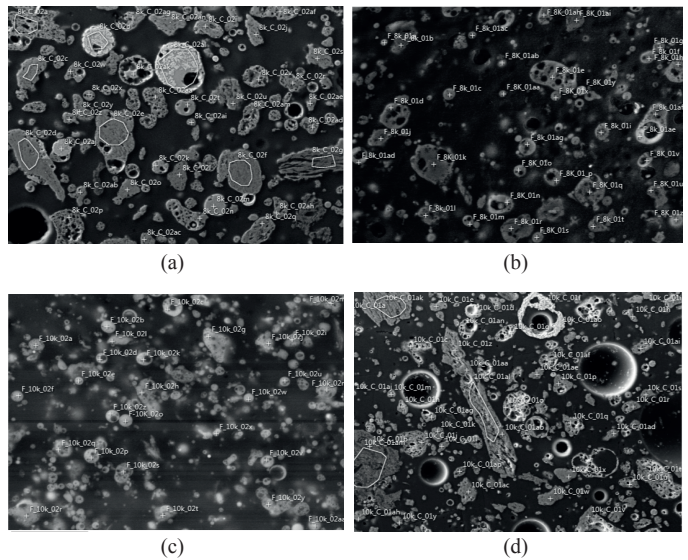


Fig. 9 Electron microscopic images at 2.5 KX magnifications for 8000 rpm fines (a), 10000 rpm fines (c), and at 500 X magnifications for 8000 rpm coarse (b), 10000 rpm coarse (d)

3.1.3 Chemical Properties

In FE-SEM images of Fig. 8 total area at lowest possible magnification of 75 X was covered to carry out EDX analyses in order to determine chemical composition of eleven elements present in fine and coarse product specimens obtained at 8000, 10000 rpm classifiers wheel speeds as shown in Table 2. It can be seen here that in all the samples of separated fly ashes, Al and Si together account for more than 80% of the particles of fly ash, in which silica is more than 50%, which makes them glassy in nature [9–11]. Further it can be seen that fine products have slightly more amount of Si in them as compared to coarse products and as the classifier's wheel speed is increased the percentage of Si increases.

The other noticeable difference in chemical composition is seen in the amount of Fe. It can be seen in Table 2 that coarse products have the higher contents of Fe as compared to fine products, this identifies that Fe rich particles also known in literature as ferrospheres or magnetospheres [33] are coarser in size and are present mostly in coarse products due to which coarse products have higher percentage of Fe. It can further be seen that as the classifiers wheel speed is increased, Fe content of coarse products decreases which is primarily due to addition of more non-Fe rich finer fraction from fine products. While coarse products contain slightly higher amounts of Ca, K, and Ti because as the Si content is reducing the contents of these elements are replacing the composition while only minor differences in contents of Mg and Cl are seen. Fly ash particles are also known to contain oxygen and carbon [34] but they have not been included in these analyses because during sample preparation for FE-SEM high amounts of oxygen is absorbed which if included in analyses would lead to higher content of oxygen determination than actually present. Samples for FE-SEM were coated with carbon due to which carbon is excluded from the analyses.

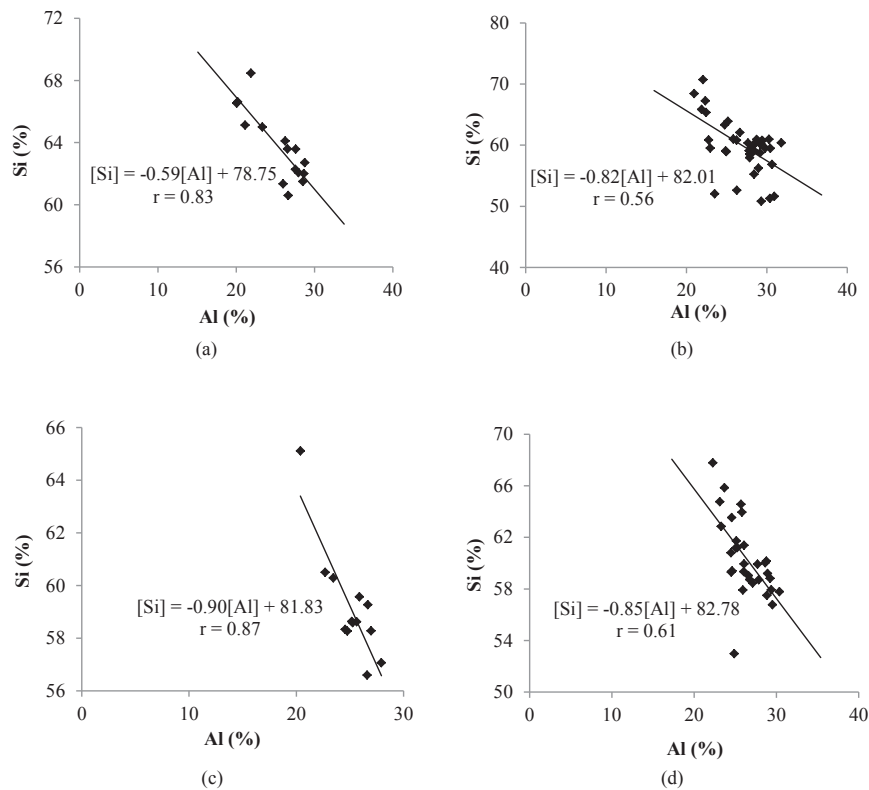


Fig. 10 EDX individual particle analyses of Fig. 9 for 8000 rpm fines (a), 8000 rpm coarse (b), 10000 rpm fines (c), and 10000 rpm coarse (d)

Table 2 Chemical composition of fine and coarse products obtained at 8000, 10000 rpm wheel speeds from EDX analyses of Fig. 8

Percentage (%)	8000 rpm fine products	8000 rpm coarse products	10000 rpm fine products	10000 rpm coarse products
Al	24.8	25.6	26.1	25.7
Si	57.9	53.1	61.1	55.9
Mg	1.09	0.95	0.92	0.89
Fe	2.48	8.67	2.64	6.27
Ca	2.44	3.14	2.07	3.61
K	3.07	4.03	3.48	4.42
Cl	1.46	1.50	1.11	0.71
Ti	0.95	1.95	0.94	1.94

3.1.4 EDX individual particle analyses

Individual particles of raw fly ash of Fig. 9 were analysed using EDX analyses with point analyses and small area analyses for the composition of Si, Al, and Fe as they are present in high percentages among the elemental composition of separated fly ashes in Table 2. It was seen from the results of the EDX individual particle analyses that majority of particles in 8000 rpm fines and 10000 rpm fines have contents of Si > 50%, Fe < 10%, and Al > 20 %, while only very few brighter particles rich in Fe were observed which showed contents of Fe between 10 and 30% which also observed by [33] are known as ferrospheres. EDX analyses for individual particles of 8000 rpm coarse and 10000 rpm coarse products also showed contents of

Si > 50%, Fe < 10%, and Al > 20 %, but a higher variation of contents were observed as compared to fine products. Higher amount of Fe rich particles, ferrospheres, were observed in coarse products having contents of Fe between 10 to 80%. As the ferrospheres have higher amount of Fe in them, which is also responsible for their higher density and during separation in the classifier the mass force exerted by peripheral velocity of classifying wheel transfers the coarser and higher density particles to the coarse products zone, therefore coarse particles contain higher amount of Fe rich ferrospheres.

The results of the analyses for Si and Al are plotted to develop a linear relationship between them as shown in Fig. 10 which was also developed by [35] to check the effect of dry separation on linear relationship between Si and Al in fly ash individual particles. The particles having contents in the range of Si > 50% and Al > 20% were plotted in Fig. 10 while particles having Fe > 10% were not plotted as they do not represent the same group of data. It can be seen here that for fine products the linear relationship equations have higher coefficient of correlation and hence a stronger linear relationship exists between them as compared to coarse products. Fine products particles are glassy particles while coarse products particles are glassy metallic particles having more contents of Fe per particle. Glassy Si rich particles have strong relationship between percentages of Si and Al [35] while glassy metallic particles rich in Fe have weak linear relationship between Si and Al.

3.2 For cement modified with raw fly ash and its separated fractions

Fig. 11(a) shows the relationship between compressive strengths of cement paste mixes of fine and coarse products at 28, 90 days of curing versus classifiers wheel speed. It can be seen here for fine products that as the classifiers wheel speed is increased compressive strength of the mixes increase. At 28 days age of specimens, increase of 3, 9, 17, 23, and 26% of compressive strength is observed for 2000, 4000, 6000, 8000 and 10000 rpm classifiers wheel speeds of fine products as compared to control specimen of raw fly ash with 60% cement replacement. Whereas at 90 days age of specimens, increase of 5, 10, 19, 29, and 33% is observed for 2000, 4000, 6000, 8000 and 10000 rpm classifiers wheel speeds of fine products as compared to control specimen.

The increase of strength at 28 days age of specimens is because of the reason that as the classifier wheel speed is increased, surface area of fine products increases as compared to control specimen which in turn increases the rate of reaction with cement particles giving higher strengths. When the particles of fly ash get smaller than the cement particles, they fill in the spaces between cement particles and hence resulting matrix show higher strengths. 90 days strength increase of specimens as compared to that at 28 days is due to the fact that fly ash particles possesses active silica that combines with calcium hydroxide produced by Portland cement hydration. After reacting they form calcium silicate hydrates which give strength to the hydrated hardened cement paste and this process only gives long term strength to cementitious composites and is well known as a pozzolanic reaction [36–37]. Further the strength increase at 90 days for increased classifiers wheel speed of specimens as compare to control specimen at 90 days is again due to the decrease in particle size and increase in surface area of fly ash particles. At 2000 rpm wheel speed coarse products have the maximum particle size and lowest surface area as determined from Fig. 5 and Fig. 6. Because of having larger particle size, lesser Si content per particle, and lesser surface area, the hydration reaction with cement of 2000 rpm coarse particles is very slow and strength attained at 28, 90 days is considerably lower as compared to control specimen of raw fly ash. It can be seen also that as the classifiers wheel speed is increased, strength of the mixes increase due to decrease in particle size. However the strength achieved for 10000 rpm coarse products is a bit less but nearly equal to the strength achieved for raw fly ash particles because the particle size of 10000 rpm coarse particles is very close to that of raw fly ash. As the age of coarse specimen is increased from 28 to 90 days pozzolanic reaction occurs between cement and fly ash particles but the reaction is slower due to the large size of coarse products therefore the strength achieved is considerably lower as compared to that of fine products.

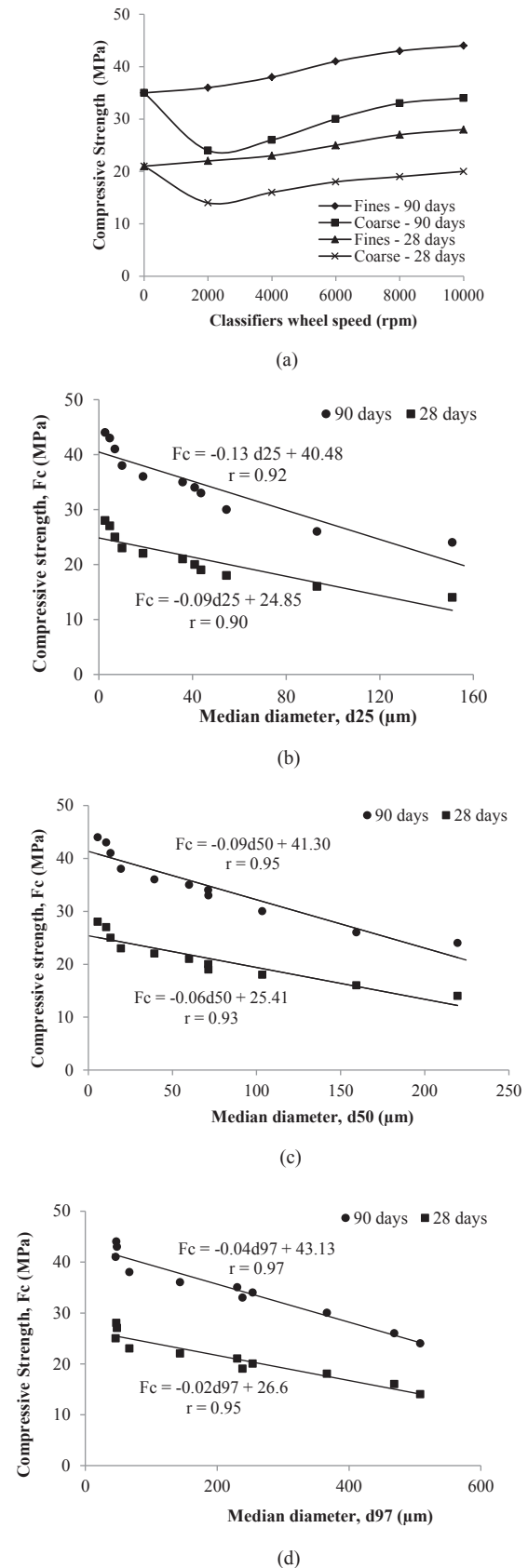


Fig. 11 Compressive strength vs classifiers wheel speed (a), for fine and coarse products at 28 and 90 days (a), Compressive strength F_c vs d_{25} (b) vs d_{50} (c), vs d_{97} (d)

Fig. 11(b), (c), and (d) shows the relationship between compressive strength at 28, 90 days and the diameters, d_{25} , d_{50} , and d_{90} for both fine and coarse products. Here it can be seen that as the particle diameters d_{25} , d_{50} , and d_{90} are increasing, compressive strength is decreasing and a linear relationship exist between the compressive strength and diameter of particles. The F_c intercept of the linear equations is increasing as the age of concrete is increased due to the combined effect of pozzolanic reaction and higher reactivity due to lesser particle size and filling of the gaps between the cement particles with fly ash fine particles. The linear equations can be used to estimate the design strength of cement – fly ash paste mixes for fly ash fine and coarse particles at 28 and 90 days. By using all three particle diameters, d_{25} , d_{50} , and d_{97} from particle size distribution analyses of brown coal raw fly ash or separated brown coal raw fly ash in equation and consequently lesser of the strength obtained out of the three equations can be used as design strength.

4 Conclusions

In this research dry separation of brown coal raw fly ash from Počerady was carried out using ultrafine air classifier. Fine and coarse products were recovered from the classifier and were tested for their properties. Further the fine and coarse products were used to prepare high volume cement paste mixes. Following conclusions are obtained from the results:

1. Air classification affected the physical properties of separated particles of raw fly ash. By increasing the wheel speed a decrease in particle diameter was observed both for fine and coarse products. It was further observed in optical microscopic images that radial size of spherical particles decreased by 75% and size of slaggy particles decreased by 97% at 10000 rpm wheel speed as compared to raw fly ash. From electron microscopy it was observed that as the wheel speed was increased from 8000 rpm to 10000 rpm, fine products changed from rounded, angular slaggy, spherical particles to mainly spherical, and very few rounded slaggy particles.
2. In EDX analyses for fine products showed high percentage of Si in them as compared to coarse products and as the wheel speed was increased, it was observed that percentage of Si increased. Whereas coarse products were found rich in Fe as compared to fine products and as the wheel speed was increased Fe content reduced. From EDX individual particle size analyses it was seen that majority of particles of fine products have contents of Si > 50%, Fe < 10%, and Al > 20%.
3. Cement – 60% fine product mixes showed higher strengths at both 28, 90 days age of curing due to higher surface area, lower particle size, higher Si available per particle for pozzolanic reaction. Moreover linear relationships were developed between the strengths and diameter of particles which can be used for design purposes.

4. As cement-fine products mixes showed higher strengths, therefore they are desired in higher quantities. In continuation of this research the coarse products can be ground/milled to reduce the particle size and SEM-EDX analyses can be used to study the milled specimens and cement paste specimens can be prepared to analyse the effects on mechanical properties.

Acknowledgement

The authors would like to thank Buildings and settlement information modelling, technology and infrastructure for sustainable development under the project TE 02000077 by TAČR.

References

- [1] Wang, SM., Zhang, CX., Chen, JD. "Utilization of Coal Fly Ash for the Production of Glass-ceramics With Unique Performances: A Brief Review." *Journal of Materials Science and Technology*. 30(12), pp. 1208–1212. 2014. DOI: [10.1016/j.jmst.2014.10.005](https://doi.org/10.1016/j.jmst.2014.10.005)
- [2] Punta, E., Lövgren, L. "Ash is a useful chemical substance - It is registered in the European Chemical Register." In: ASH 2012. Stockholm, Sweden Jan. 25-27, 2012. URL: http://www.varmeforsk.se/files/program/askor/2_punta_.pdf
- [3] Blissett, R. S., Rowson, N. A. "A review of the multi-component utilization of coal fly ash." *Fuel*. 97, pp. 1–23. 2012. DOI: [10.1016/j.fuel.2012.03.024](https://doi.org/10.1016/j.fuel.2012.03.024)
- [4] Cez Group. URL: <http://www.cez.cz/en/power-plants-and-environment/coal-fired-power-plants.html>. Accessed 3 September, 2015.
- [5] Ahmaruzzaman, M. "A review on the utilization of fly ash." *Progress in Energy and Combustion Science*. 36(3), pp. 327–363. 2010. DOI: [10.1016/j.pecc.2009.11.003](https://doi.org/10.1016/j.pecc.2009.11.003)
- [6] Ishito, K., Akiyama, S., Tanaka, Z. "Improvement of grinding and classifying performance using a closed-circuit system." *Advanced Powder Technology*. 13(4), pp. 363–375. 2002. DOI: [10.1163/156855202320536016](https://doi.org/10.1163/156855202320536016)
- [7] Kiattikomol, K., Jaturapitakkul, C., Songpiriyakij, S., Chutubtim, S. "A study of ground coarse fly ashes with different fineness from various sources as pozzolanic materials." *Cement and Concrete Composites*. 23(4-5), pp. 335–343. 2001. DOI: [10.1016/S0958-9465\(01\)00016-6](https://doi.org/10.1016/S0958-9465(01)00016-6)
- [8] Zhang, C. F., Qiang, Y., Sun, J. M. "Characteristics of particulate matter from emissions of four typical coal-fired power plants in China." *Fuel Processing Technology*. 86(7), pp. 757–768. 2005. DOI: [10.1016/j.fu-proc.2004.08.006](https://doi.org/10.1016/j.fu-proc.2004.08.006)
- [9] Kutchako, B. G., Kim, A. G. "Fly ash characterization by SEM-EDS." *Fuel*. 85(17), pp. 2537–2544. 2006. DOI: [10.1016/j.fuel.2006.05.016](https://doi.org/10.1016/j.fuel.2006.05.016)
- [10] Medina, A., Gamero, P., Querol, X., Moreno, N., De León, B., Almanza, M., Vargas, G., Izquierdo, M., Font, O. "Fly ash from a Mexican mineral coal I: Mineralogical and chemical characterization." *Journal of Hazardous Materials*. 181(1-3), pp. 82–90. 2010. DOI: [10.1016/j.jhazmat.2010.04.096](https://doi.org/10.1016/j.jhazmat.2010.04.096)
- [11] Zhao, JH., Wang, DM., Wang, XG., Liao, SC., Lin, H. "Ultrafine grinding of fly ash with grinding aids: Impact on particle characteristics of ultrafine fly ash and properties of blended cement containing ultrafine fly ash." *Construction and Building Materials*. 78, pp. 250–259. 2015. DOI: [10.1016/j.conbuildmat.2015.01.025](https://doi.org/10.1016/j.conbuildmat.2015.01.025)
- [12] Pedersen, K. H., Jensen, A. D., Skjoth-Rasmussen, MS., Dam-Johansen, K. "A review of the interference of carbon containing fly ash with air entrainment in concrete." *Progress in Energy and Combustion Science*. 34(2), pp. 135–154. 2008. DOI: [10.1016/j.pecc.2007.03.002](https://doi.org/10.1016/j.pecc.2007.03.002)

- [13] Kolay, P. K., Singh, D. N. "Physical, chemical, mineralogical, and thermal properties of cenospheres from an ash lagoon." *Cement and Concrete Research*. 31(4), pp. 539-542. 2001. DOI: [10.1016/S0008-8846\(01\)00457-4](https://doi.org/10.1016/S0008-8846(01)00457-4)
- [14] Ngu, LL., Wu, H., Zhang, DK. "Characterization of Ash Cenospheres in Fly Ash from Australian Power Stations." *Energy & Fuels*. 21(6), pp. 3437-3445. 2007. DOI: [10.1021/ef700340k](https://doi.org/10.1021/ef700340k)
- [15] Kolay, P. K., Bhusal, S. "Recovery of hollow spherical particles with two different densities from coal fly ash and their characterization." *Fuel*. 117, pp. 118-124. 2014. DOI: [10.1016/j.fuel.2013.09.014](https://doi.org/10.1016/j.fuel.2013.09.014)
- [16] Hirajima, T., Oosako, Y., Nonaka, M., Petrus, H. T. B. M., Sasaki, K., Ando, T. "Recovery of hollow and spherical particles from coal fly ash by wet separation process." *Journal of MMLJ*. 124(12), pp. 878-884. 2008. DOI: [10.2473/journalofmmlj.124.878](https://doi.org/10.2473/journalofmmlj.124.878)
- [17] Vassilev, S. V., Vassileva, C. G. "Geochemistry of coals, coal ashes and combustion wastes from coal-fired power stations." *Fuel Processing Technology*. 51(1-2), pp. 19-45. 1997. DOI: [10.1016/S0378-3820\(96\)01082-X](https://doi.org/10.1016/S0378-3820(96)01082-X)
- [18] "Panki Katra fly ash contamination" URL: <http://www.blacksmithinstitute.org/projects/display/114>
- [19] Shapiro, M., Galperin, V. "Air classification of solid particles: a review." *Chemical Engineering and Processing: Process Intensification*. 44(2), pp. 279-285. 2005. DOI: [10.1016/j.ccep.2004.02.022](https://doi.org/10.1016/j.ccep.2004.02.022)
- [20] Hirajima, T., Petrus, H. T. B. M., Oosako, Y., Nonaka, M., Sasaki, K., Ando, T. "Recovery of cenospheres from coal fly ash using a dry separation process: Separation estimation and potential application." *International Journal of Mineral Processing* 95(1-4), pp. 18-24. 2010. DOI: [10.1016/j.minpro.2010.03.004](https://doi.org/10.1016/j.minpro.2010.03.004)
- [21] Petrus, H. T. B. M., Hirajima, Tsuyoshi, Oosako, Y., Nonaka, M., Sasaki, K., Ando, T. "Performance of dry-separation processes in the recovery of cenospheres from fly ash and their implementation in a recovery unit." *International Journal of Mineral Processing*. 98(1-2), pp. 15-23. 2011. DOI: [10.1016/j.minpro.2010.09.002](https://doi.org/10.1016/j.minpro.2010.09.002)
- [22] Nied, R. "CFS-HD: A new classifier for fine classification with high efficiency." *International journal of Mineral Processing*. 44-45, pp. 723-731. 1996. DOI: [10.1016/0301-7516\(95\)00078-X](https://doi.org/10.1016/0301-7516(95)00078-X)
- [23] Allardice, D. J. "The water in brown coal." In: *The Science of Victorian Brown Coal. Structure, Properties and Consequences for Utilization*. (Durie, R. A. Ed.), pp. 103-150. Butterworth-Heinemann Ltd, Oxford. 1991.
- [24] Malvern Instruments Ltd. URL: <http://www.malvern.com/en/products/measurement-type/particle-size/>. Accessed 4 January, 2015.
- [25] Horiba Scientific. "A guidebook to particle size analysis." URL: https://www.horiba.com/fileadmin/uploads/Scientific/eMag/PSA/Guidebook/pdf/PSA_Guidebook.pdf. Accessed 5 January, 2015.
- [26] Hosokawa micron powder systems. URL: <http://www.hmicronpowder.com/products/product/alpine-afg-fluidized-bed-jet-mill>. Accessed 21 August, 2015.
- [27] Ceramic Industry. URL: <http://www.ceramicindustry.com/articles/84108-product-profile-high-throughput-with-a-fine-grind>. Accessed 5 January, 2015
- [28] Itskos, S. G., Itskos, S., Koukouzas, N. "The effect of the particle size differentiation of lignite fly ash on cement industry applications." In: World of Coal Ash (WOCA) Conference 2009. Lexington, KY, USA, May 4-7. 2009.
- [29] Hrnčířova, M., Pospíšil, J., Špilaček, M. "Size analysis of solid particles using laser diffraction and sieve analysis." *Engineering Mechanics*. 20(3-4), pp. 309-318. 2013.
- [30] Durdziński, P. T., Dunant, C. F., Haha, M. B., Scrivener, K. L. "A new quantification method based on SEM-EDS to assess fly ash composition and study the reaction of its individual components in hydrating cement paste." *Cement and Concrete Research*- 73, pp. 111-122. 2015. DOI: [10.1016/j.cemconres.2015.02.008](https://doi.org/10.1016/j.cemconres.2015.02.008)
- [31] Goodarzi, F. "Morphology and chemistry of fine particles emitted from a Canadian coal-fired power plant." *Fuel*. 85(3), pp. 273-280. 2006. DOI: [10.1016/j.fuel.2005.07.004](https://doi.org/10.1016/j.fuel.2005.07.004)
- [32] Chen, Y., Shah, N., Huggins, FE., Huffman, GP., Dozier, A. "Characterization of ultrafine coal fly ash particles by energy-filtered TEM." *Journal of Microscopy*. 217(Pt. 3), pp. 225-234. 2005. DOI: [10.1111/j.1365-2818.2005.01445.x](https://doi.org/10.1111/j.1365-2818.2005.01445.x)
- [33] Valentim, B., Shreya, N., Paul, B., Gomes, C. S., Sant'Ovaia, H., Guedes, A., Ribeiro, J., Flores, D., Pinho, S., Suárez-Ruiz, I., Ward, C. R. "Characteristics of ferrospheres in fly ashes derived from Bokaro and Jharia (Jharkand, India) coals." *International Journal of Coal Geology* 153, pp. 52-74. 2016. DOI: [10.1016/j.coal.2015.11.013](https://doi.org/10.1016/j.coal.2015.11.013)
- [34] Deng, S., Shu, Y., Li, SB., Tian, G., Huang, JY., Zhang, F. "Chemical forms of the fluorine, chlorine, oxygen and carbon in coal fly ash and their correlations with mercury retention." *Journal of Hazardous Materials*. 301, pp. 400-406. 2016. DOI: [10.1016/j.jhazmat.2015.09.032](https://doi.org/10.1016/j.jhazmat.2015.09.032)
- [35] Anshits, N., Mikhailova, O. A., Salanov, A. N., Anshits, A. G. "Chemical composition and structure of the shell of fly ash non-perforated cenospheres produced from the combustion of the Kuznetsk coal (Russia)." *Fuel*. 89(8), pp. 1849-1862. 2010. DOI: [10.1016/j.fuel.2010.03.049](https://doi.org/10.1016/j.fuel.2010.03.049)
- [36] Massazza, F., Costa, U. "Factors determining the development of mechanical strength in lime - pozzolana pastes." In: Proceedings of the XII Conference on Silicate Industry and Silicate Science, Budapest, Jun. 6-11. 1977. Vol. 1. p. 537.
- [37] Rong, Z. D., Sun, W., Xiao, H. J., Wang, W. „Effect of silica fume and fly ash on hydration and microstructure evolution of cement based composites at low water-binder ratios." *Construction and Building Materials*. 51 pp. 446-450. 2014. DOI: [10.1016/j.conbuildmat.2013.11.023](https://doi.org/10.1016/j.conbuildmat.2013.11.023)